

# Description of *Triatoma huehuetenanguensis* sp. n., a potential Chagas disease vector (Hemiptera, Reduviidae, Triatominae)

Raquel Asunción Lima-Cordón<sup>1</sup>, María Carlota Monroy<sup>2</sup>, Lori Stevens<sup>1</sup>,  
Antonieta Rodas<sup>2</sup>, Gabriela Anaité Rodas<sup>2</sup>, Patricia L. Dorn<sup>3</sup>, Silvia A. Justí<sup>1,4,5</sup>

**1** Department of Biology, University of Vermont, Burlington, Vermont, USA **2** The Applied Entomology and Parasitology Laboratory at Biology School, Pharmacy Faculty, San Carlos University of Guatemala, Guatemala **3** Department of Biological Sciences, Loyola University New Orleans, New Orleans, Louisiana, USA **4** Walter Reed Biosystematics Unit, Smithsonian Institution Museum Support Center, Maryland, USA **5** Walter Reed Army Institute of Research, Silver Spring, MD, USA

Corresponding author: Raquel Asunción Lima-Cordón ([raqueasu7@gmail.com](mailto:raqueasu7@gmail.com))

Academic editor: G. Zhang | Received 6 June 2018 | Accepted 4 November 2018 | Published 28 January 2019

<http://zoobank.org/14B0ECA0-1261-409D-B0AA-3009682C4471>

**Citation:** Lima-Cordón RA, Monroy MC, Stevens L, Rodas A, Rodas GA, Dorn PL, Justí SA (2019) Description of *Triatoma huehuetenanguensis* sp. n., a potential Chagas disease vector (Hemiptera, Reduviidae, Triatominae). ZooKeys 820: 51–70. <https://doi.org/10.3897/zookeys.820.27258>

## Abstract

A new species of the genus *Triatoma* Laporte, 1832 (Hemiptera, Reduviidae) is described based on specimens collected in the department of Huehuetenango, Guatemala. *Triatoma huehuetenanguensis* sp. n. is closely related to *T. dimidiata* (Latreille, 1811), with the following main morphological differences: lighter color; smaller overall size, including head length; and width and length of the pronotum. Natural *Trypanosoma cruzi* (Chagas, 1909) infection, coupled with its presence in domestic habitats, makes this species a potentially important vector of *Trypanosoma cruzi* in Guatemala.

## Keywords

Chagas disease vector, *Triatoma dimidiata* s.l., *Trypanosoma cruzi*

## Introduction

As of 2010, more than a million cardiomyopathy cases in Latin America were caused by Chagas disease (WHO 2015) due to the parasite *Trypanosoma cruzi* (Chagas, 1909).

This illness is mainly transmitted through the infected feces of insects of the subfamily Triatominae (Hemiptera: Reduviidae). Known colloquially as kissing bugs, the group is currently divided into five tribes and 15 genera (Justi and Galvao 2017; World Health Organization 2015; Schofield and Galvao 2009). Among these, *Triatoma* Laporte, 1832, *Panstrongylus* Berg, 1879 and *Rhodnius* Stål, 1859 (the first two belonging to the tribe Triatomini and the third genera belonging to Rhodniini) are the most epidemiologically relevant for Chagas transmission (WHO 2002).

The genus *Triatoma* is the most diverse, comprising over half of the described Triatominae species (Justi and Galvao 2017; Schofield and Galvao 2009). *Triatoma dimidiata* (Latreille, 1811), the most important Chagas disease vector in Central America, is in fact a species complex including at least three independently evolving lineages initially identified by sequences of nuclear (internal transcribed spacer, ITS-2) and the mitochondrial marker cytochrome b (cytb) (Bargues et al. 2008; Dorn et al. 2016), and later confirmed by phylogenetic studies using SNPs and species delimitation, obtained by a reduced representation genome genotyping by sequencing (GBS) approach (Justi et al. 2018). These studies recovered *T. dimidiata* as four lineages: groups 1 – 4, which appeared to include at least three species: groups 1 and 2 – *T. dimidiata* s. str., group 3 – *Triatoma* sp. aff. *dimidiata*, and group 4 – *Triatoma* sp. aff. *dimidiata* cave (Bargues et al. 2008, Dorn et al. 2016, Justi et al. 2018). The last of these taxa, *Triatoma* sp. aff. *dimidiata* cave (= group 4) was recently described as a new species, *Triatoma mopan* Dorn, Justi & Dale, 2018.

In this study, we formally describe *Triatoma* sp. aff. *dimidiata* (group 3) based on morphological and molecular data and name it *Triatoma huehuetenanguensis* sp. n., after the type locality in Guatemala.

## Materials and methods

### Sampling

A total of 39 *Triatoma* specimens was obtained between April 2015 and May 2016 through community participation in the department of Huehuetenango, Guatemala and given to personnel from the Ministry of Health of Huehuetenango who shipped them to the Applied Entomology and Parasitology Laboratory (LENAP), at San Carlos University in Guatemala City. At LENAP the specimens were preserved in 95% ethanol and 5% glycerol and stored at room temperature. Specimens were identified as *T. dimidiata* using the taxonomic key for the genus *Triatoma* published by Lent and Wygodzinsky (1979).

Three females and three males were left intact to comprise the type series used for the morphological description of the new species. DNA was extracted from the remaining 20 by Justi et al. (2018) and tested for infection with *T. cruzi*. Justi et al. (2018) previously recovered all 20 specimens within the same highly supported monophyletic clade named *Triatoma* sp. aff. *dimidiata* based on genome SNP phylogenies.

## Morphological characterization

Since there is no known holotype for *T. dimidiata* (Latreille, 1811), the characterization of the new species was done following the same methodology as Dorn et al. (2018) for the description of *T. mopan*.

Based on (Lent and Wygodzinsky 1979), 17 morphological traits were measured from the type series and an additional 13 specimens and from 15 female and ten male *Triatoma dimidiata* s. str. (group 1–2) from Huehuetenango, Jutiapa and Chiquimula in Guatemala. These 25 *Triatoma dimidiata* s. str. specimens were preserved under the same conditions as the new species (95% ethanol and 5% glycerol). Measurements of the morphological traits were performed using a Nikon stereoscope Model SMZ-1B (see Suppl. material 1: morphological measurements). The morphological traits were:

- |                             |  |
|-----------------------------|--|
| (1) total length,           | (7) ante-ocular region,                    |
| (2) width of the pronotum,  | (8) post-ocular region,                    |
| (3) width of the abdomen,   | (9) width of the eye,                      |
| (4) head length,            | (10) synthlipsis,                          |
| (5) width across eyes,      | (11–14) each of the four antennomeres, and |
| (6) length of the pronotum, | (15–17) each of the three labial articles. |

Because of unequal sample sizes for each group (*T. dimidiata* s. str. and the new species), an unpaired t test was used to compare the means of each of the 17 morphological traits in the two groups (JMP Pro version 13.0.0).

Insects were photographed using a Visionary Digital BK Laboratory System, a Canon 5D camera, 65 mm macro zoom lens. Photo stacks of 25–45 slices were compiled using Helicon Focus 5.3 and the image edited to balance light quality, remove background blemishes, and provide a scale on Photoshop CS6.

## *Trypanosoma cruzi* infection

Natural infection by *T. cruzi* was tested by PCR on genomic DNA extracted from the last three segments of the specimens' abdomen. DNA was extracted using Qiagen DNeasy blood and tissue kit, following the manufacturer's tissue protocol for the first two steps, blood protocol for subsequent steps and an additional incubation (65 °C for 10 min, followed by 95 °C for 5 min.). Primers and PCR assay conditions were used as previously described (Moser et al. 1989).

## Molecular phylogenetic analysis

In order to: (a) keep the type series intact, (b) confirm that any specimens that share the same phenotype with the type series belong to *Triatoma* sp. aff *dimidiata*, and (c)

to determine the relationship with the other groups of *T. dimidiata* s.l., ITS-2 and cytB were sequenced for two out of the 20 *Triatoma* sp. aff. *dimidiata* specimens studied by Justi et al. (2018). Sequencing was performed as previously described by Dorn et al. (2016). For comparison, ITS-2 and cytB sequences including representatives from all *T. dimidiata* s.l. groups were retrieved from GenBank (Table 1) and aligned using the algorithm Q-INS-I implemented in the online MAFFT version 7 (Kato et al. 2017) and ClustalW (Larkin et al. 2007) implemented on MEGA v. 6 (Tamura et al. 2013), respectively. Maximum likelihood phylogenies were reconstructed independently for each of the genes using PhyML v.3.1 (Guindon and Gascuel 2003), with 100 bootstrap replicates. The best fit model for each gene, according to the AIC criterion, estimated using JModeltest (Darriba et al. 2015), were model HKY+I for ITS-2 and HKY + G for cytB. *Triatoma infestans* (Klug, 1834) was used as the outgroup. Both phylogenies were reconstructed using the same specimens for both markers, as indicated in the original studies. Phylogenies were plotted as mirror images using the function cophyloplot, from the package ape (Paradis et al. 2004), in R (R Development Core Team, 2013). Specimens photos and clade highlights were inserted using Adobe Photoshop CC 2108.

## Distribution map

Reported confirmed distributions of *T. huehuetenanguensis* sp. n. and specimens previously identified as *Triatoma* sp. aff. *dimidiata*, by molecular means were compiled (Table 2, Fig. 1) and GPS coordinates and altitudes were inferred using Google Maps. Localities were plotted on a map of Central America, using the packages plyr (Wickham 2011), raster (Hijmans 2012) and maps (Becker 2017) available in R (R Development Core Team 2008). The script is available in a supplementary file (Suppl. material 2: Script Huehuetenango map).

## Taxonomy

**Family Reduviidae Latreille, 1807**

**Subfamily Triatominae Jeannel, 1919**

**Genus *Triatoma* Laporte, 1832**

***Triatoma huehuetenanguensis* Lima-Cordón & Justi, sp. n.**

<http://zoobank.org/F785B1DC-4946-4FAE-BA5D-D36CA413C67B>

**Material. Holotype:** Male. GUATEMALA: Huehuetenango, La Democracia, Aldea Chamuxu, coordinates: 15.6333/-91.8667, 2 May 2016, C. Monroy and A. Rodas, National Museum of Natural History, Smithsonian Institution (voucher: USNM-ENT01241940). **Paratypes:** One female. GUATEMALA: Huehuetenango, San Pedro Necta, Caserio San Juan, coordinates 15.5/-91.76667, 1 June 2016, C. Mon-

**Table 1.** *Triatoma* specimens used to reconstruct the phylogeny, including collection location, sample identification, and GenBank accession numbers.

Taxon	Locality	Sequence ID	ITS-2	Cyt b
<i>T. dimidiata</i>	1	Sta. Theresa, Toledo, Belize	DQ871354	FJ197155
	10	Caserío la Bendición, Santa Ana, El Salvador	AM286693	JN585881
	11	Caserío la Bendición, Santa Ana, El Salvador	AM286693	JN585881
	12	Caserío la Bendición, anta Ana, El Salvador	AM286693	JN585881
	13	Caserío la Bendición, Santa Ana, El Salvador	AM286695	JN585881
	14	Caserío la Bendición, Santa Ana, El Salvador	KT874438	JN585881
	15	Sto. Tomás, Sto. Domingo, Heredia, Costa Rica	AM286693	JN585893
	16	Sto. Tomás, Sto. Domingo, Heredia, Costa Rica	AM286693	JN585894
	17	Sto. Tomás, Sto. Domingo, Heredia, Costa Rica	AM286693	JN585894
	18	Angeles, San Rafael, Heredia, Costa Rica	KF192843	JN585894
	19	Sto. Tomás, Sto. Domingo, Heredia, Costa Rica	KT874433	JN585895
	2	Mérida, Yucatán, Mexico	FJ197146	FJ197157
	20	Colombia	AM286703	KT998309
	21	Colombia	AM286703	KT998309
	22	Colombia	AM286704	KT998309
	23	Colombia	KF192845	KT998310
	24	Lanquin, Alta Verapaz, Guatemala	AM286702	KT998313
	25	Lanquin, Alta Verapaz, Guatemala	AM286702	KT998314
	26	El Lodo Negro, Intibuca, Honduras	AM286694	KT998315
	27	El Masical, San Antonio, Copán, Honduras	AM286694	KT998316
	28	El Masical, San Antonio, Copán, Honduras	AM286695	KT998316
	29	Caserío la Bendición, Santa Ana, El Salvador	AM286693	KT998317
	3	Lanquin, Alta Verapaz, Guatemala	AM286694	JN585861
	30	Caserío la Bendición, Santa Ana, El Salvador	AM286696	KT998318
	31	El Lodo Negro, Intibuca, Honduras	AM286695	KT998319
	32	El Masical, San Antonio, Copán, Honduras	AM286694	KT998320
	33	El Lodo Negro, Intibuca, Honduras	AM286693	KT998321
	34	El Lodo Negro, Intibuca, Honduras	KT874435	KT998321
	35	El Lodo Negro, Intibuca, Honduras	KT874437	KT998321
	36	El Masical, San Antonio, Copán, Honduras	AM286693	KT998322
	37	El Masical, San Antonio, Copán, Honduras	KT874436	KT998322
	38	El Lodo Negro, Intibuca, Honduras	AM286693	KT998325
	39	El Lodo Negro, Intibuca, Honduras	AM286694	KT998325
	4	Lanquin, Alta Verapaz, Guatemala	AM286702	JN585861
	40	El Lodo Negro, Intibuca, Honduras	AM286695	KT998325
	41	El Masical, San Antonio, Copán, Honduras	KT874434	KT998325
	42	Caserío la Bendición, Santa Ana, El Salvador	AM286693	KT998327
	43	Angeles, San Rafael, Heredia, Costa Rica	AM286693	KT998328
	44	Sto. Tomás, Sto. Domingo, Heredia, Costa Rica	KT874432	KT998330
	45	Angeles, San Rafael, Heredia, Costa Rica	KF192844	KT998331
	46	San Pedro Columbia, Toledo district, Belize	FJ197153	FJ197154
	5	Caserío la Bendición, Santa Ana, El Salvador	AM286693	JN585881
	6	Caserío la Bendición, Santa Ana, El Salvador	AM286693	JN585881
	7	Caserío la Bendición, Santa Ana, El Salvador	AM286693	JN585881
	8	Caserío la Bendición, Santa Ana, El Salvador	AM286693	JN585881
9	Caserío la Bendición, Santa Ana, El Salvador	AM286693	JN585881	
<i>T. huehuetenanguensis</i>	A10227	Caserío San Pedro, Huehuetenango, Guatemala	MG947606	MG951755
	A10058	Comunidad El Rosario, Huehuetenango, Guatemala	MG947605	MG951754
<i>T. sp. aff dimidiata</i>	1	Calla Creek, Cayo District, Belize	FJ197152	FJ197156
	2	Mérida, Yucatán, Mexico	FJ197150	FJ197158
	3	Mérida, Yucatán, Mexico	FJ197147	FJ197159
	4	Teya, Yucatán, Mexico	KT874439	KT998296
<i>T. mopan</i>	1	Río Frio Cave, Cayo District, Belize	KF192846	JN585883
	2	Río Frio Cave, Cayo District, Belize	KF192847	JN585884
<i>T. infestans</i>			AJ576054	JN006799

**Table 2.** Localities where *T. huehuetenanguensis* (*Triatoma* sp. aff. *dimidiata*) was reported and corresponding longitude, latitude and altitude (meters above the sea level [m a.s.l.]).

Locality	Longitude	Latitude	Altitude (m a.s.l.)	Reference
Barrio La Unión, Huehuetenango, Guatemala	-91.771511	16.261333	918	Justi et al. 2018
Calkiní, Campeche, Mexico	-90.0505156	20.3707299	16.61	Dorn et al. 2016
Calla Creek, Cayo District, Belize	-89.1338271	17.1257479	69.55	Dorn et al. 2016
Casario San Pedro, Cuilco, Huehuetenango, Guatemala	-91.966667	15.4	1144.82	This study
Chablekal, Merida, Yucatan, Mexico	-89.5756987	21.0961842	8.9	Bargues et al. 2008
Chapalá, Cuilco, Huehuetenango, Guatemala	-91.966667	15.4	1144.82	This study
Comunidad El Rosario, Huehuetenango, Guatemala	-91.47826	15.31871	1889.08	Justi et al. 2018
	-91.966667	15.4	1144.82	This study
Cozumel island, Quintana Roo, Mexico	-86.9223432	20.4229839	14.02	Bargues et al. 2008
El Escondido, La Democracia, Huehuetenango, Guatemala	-91.887456	15.622212	895.51	Justi et al. 2018
El Paraiso, Yoro, Honduras	-87.016667	14.983333	1753.10	Bargues et al. 2008
El Triunfo, Poptún, Petén, Guatemala	-89.4221967	16.3279338	521.54	Dorn et al. 2016
	-89.4221967	16.3279338	521.54	Dorn et al. 2016
Holbox island, Quintana Roo, Mexico	-87.2866995	21.5308421	3	Bargues et al. 2008
Ixchehux, Jacaltenango, Huehuetenango, Guatemala	-91.759167	15.722778	959.91	Justi et al. 2018
Izamal, Yucatan, Mexico	-89.0227126	20.9299997	14	Bargues et al. 2008
Las Galeras, San Antonio, Huehuetenango, Guatemala	-91.771362	15.651625	1031.98	Justi et al. 2018
	-91.771362	15.651625	1031.98	Justi et al. 2018
Los Chucles, La Democracia, Huehuetenango, Guatemala	-91.88062	15.62151	895.51	Justi et al. 2018
Los Encuentros, Poptún, Petén, Guatemala	-89.4221967	16.3279338	512.87	Dorn et al. 2016
Mérida, Yucatán, Mexico	-89.59258	20.96737	10.72	Dorn et al. 2016
Palenque, Chiapas, Mexico	-91.9930466	17.5109792	67.08	Bargues et al. 2008
Paraiso, Yucatan, Mexico	-89.638845	21.0108241	9.97	Bargues et al. 2008
Sabener, Cuilco, Huehuetenango, Guatemala	-91.966667	15.4	1144.82	Justi et al. 2018
San Luis, Petén, Guatemala	-89.4399388	16.2000032	381.78	Dorn et al. 2016
Subirama, Yoro, Honduras	-87.4480115	15.2021628	843.60	Bargues et al. 2008
Teya, Yucatán, Mexico	-89.5220406	20.9358411	12.87	Dorn et al. 2016
Yaxha, Peten, Guatemala	-89.4024797	17.0734395	258.80	Bargues et al. 2008
Yaxkukul, Yucatan, Mexico	-89.4204	21.0615692	14.78	Bargues et al. 2008

roy and A. Rodas, National Museum of Natural History, Smithsonian Institution, (voucher: USNMNT01241941). Two males. GUATEMALA: Huehuetenango, La Democracia, Aldea Chamuxu, coordinates: 15.6333/-91.8667, 2 May 2016, C. Monroy and A. Rodas, and GUATEMALA: Huehuetenango, San Antonio Huista, Canton Reforma, coordinates: 15.65/-91.7667, May 2016, C. Monroy and A. Rodas, Applied Entomology and Parasitology Laboratory- LENAP (ID: A10723 and A10685, respectively). Two females. GUATEMALA: Huehuetenango, La Democracia, Aldea Chamuxu, coordinates: 15.6333/-91.8667, 28 May 2016, C. Monroy and A. Rodas, and GUATEMALA: Huehuetenango, La Democracia, Aldea Chamuxu, coordinates: 15.6333/-91.8667, 28 May 2016, C. Monroy and A. Rodas, Applied Entomology and Parasitology Laboratory- LENAP (ID: A10800 and A10673, respectively).

**Etymology.** The name *Triatoma huehuetenanguensis* is in reference to the locality (Department of Huehuetenango, Guatemala) where the holotype and paratype specimens were collected.

**Differential diagnosis.** Specimens of *T. huehuetenanguensis* are classified as *T. dimidiata* following the key published by Lent and Wygodzinsky (1979). On closer examination, *T. huehuetenanguensis* differs from *T. dimidiata* in the following diagnos-

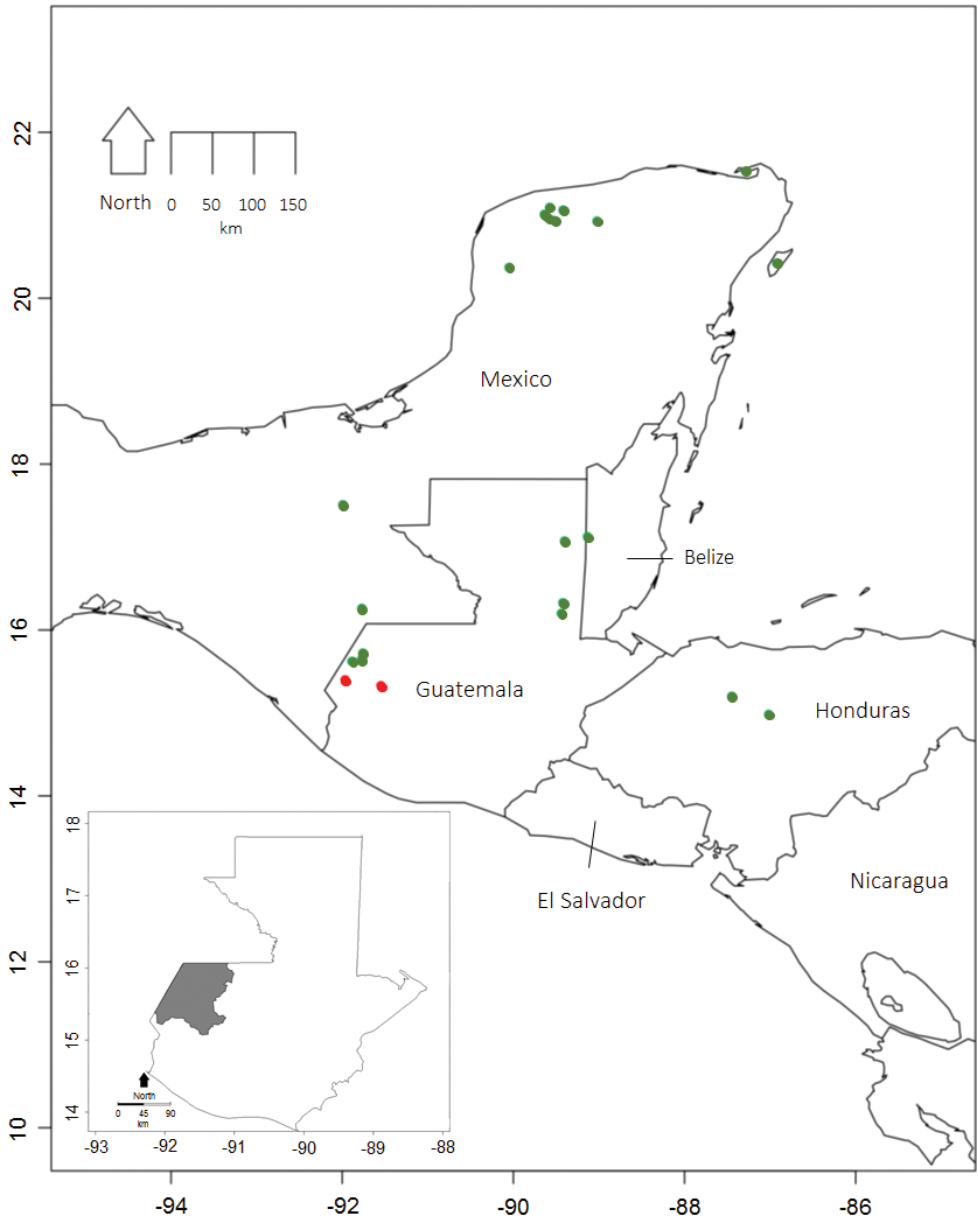


**Figure 1.** *Triatoma huehuetenanguensis* distribution map based on Bargues et al. (2008), Dorn et al. (2016), Justi et al. (2018) and this study. The red spots designate the places where the holotype and paratypes were collected, the green points refer to the locations where *T. sp. aff. dimidiata* was previously reported. Map insert highlights the department of Huehuetenango, where *T. huehuetenanguensis* holotype and paratypes were collected.

tic characters: overall color of connexivum, color of head pilosity, ocelli, setae in the second antennomere, anterolateral angles, labial articles joints, setae in the abdomen, spiracles, and female and male terminalia.

In contrast to the connexivum and corium color of *T. dimidiata* (pale yellow to orange yellow), *T. huebuetenanguensis* is brown, with connexivum and corium from yellow to pale yellow. The ventral color in *T. huebuetenanguensis* is light yellow, while in *T. dimidiata* it is piceous or black (Fig. 2). The setae around the abdomen are less dense in *T. huebuetenanguensis* when compared to *T. dimidiata*. In *T. huebuetenanguensis*, the spiracles are adjacent to the connexival suture, while in *T. dimidiata*, the spiracles are close but not adjacent to the connexival suture. In addition, spiracles are surrounded by a dark spot in *T. dimidiata*, while the spot is absent in *T. huebuetenanguensis* (Fig. 5). The first antennomere in *T. huebuetenanguensis* does not reach the apex of the head, whereas in *T. dimidiata*, it does. The setae in the second antennomere of *T. huebuetenanguensis* are not as dense as in *T. dimidiata* (Fig. 3). Anterolateral angles are laterally oriented in *T. huebuetenanguensis*, while in *T. dimidiata* they are anterolaterally oriented. The three labial articles of *T. huebuetenanguensis* are light colored while in *T. dimidiata* they are dark, similar to the dark body color. The joint of each of the labial articles are pale yellow only in *T. huebuetenanguensis* (Fig. 3). The collar is relatively thicker in *T. huebuetenanguensis* compared with *T. dimidiata*. The scutellum is rugose in both, *T. dimidiata* and *T. huebuetenanguensis*. However, the central scutellum area in *T. huebuetenanguensis* is more depressed as compared with *T. dimidiata* (Fig. 4). Legs in *T. huebuetenanguensis* with 1 + 1 subapical denticles, sometimes with a very small apical denticle on fore and/or mid-femora. Females sometimes with only one subapical denticle or a callosity, slightly lighter than the tegument on its proximal side. Fore and mid-femora of both males and females with lighter ventral subapical band, ranging from almost imperceptible to yellow.

The terminalia in males of *T. huebuetenanguensis* is almost square-shaped and darker than the rest of the tegument, presenting sparse dark pilosity, while in *T. dimidiata* it is ovoid and dark, presenting abundant dark pilosity. Posterior margin of urosternite VIII convex on *T. dimidiata* and almost straight in *T. huebuetenanguensis*. Posterior margin of urosternite IX slightly sinuous and not exceeding the abdomen on *T. huebuetenanguensis*, convex and exceeding the abdomen on *T. dimidiata*. Female terminalia in both species is triangle-shaped with very dark and dense pilosity. However, in *T. huebuetenanguensis* it is pale and very pointed while, in *T. dimidiata* it has rounded apex and is dark colored. Posterior margin of sternite VII sinuous on *T. dimidiata* and very sinuous in *T. huebuetenanguensis*; gonocoxite VIII (Gc8) pointed on *T. huebuetenanguensis* and rounded on *T. dimidiata*; gonapophysis VIII (Gp8) is wider than long in *T. huebuetenanguensis* compared to *T. dimidiata*. Gonocoxite IX (Gc9) strongly expanded exceeding the abdomen in *T. huebuetenanguensis* compared to *T. dimidiata* (Fig. 6).

**Description.** Overall color brown, connexivum, and corium yellow to light yellow. Pilosity short, distinctively yellow, covering whole body, except male and female terminalia, where pilosity is brown.

Total length, male 22.5–26.5 mm, female 22.2–29.3 mm; pronotum width, male 4.9–6.2 mm, females 4.9–6.4 mm; pronotum length, male 3.7–4.2 mm, female 3.4–4.5 mm (Table 3).

**Table 3.** Means and standard deviation (in parenthesis) of 17 morphological traits taken from *T. huehuetenanguensis* sp. n. and *T. dimidiata*.

Morphological character	<i>T. dimidiata</i>		<i>T. huehuetenanguensis</i>		
	♀ (mm)	♂ (mm)	♀ (mm)	♂ (mm)	
<b>Total length</b> <sup>†</sup>	33.7 (1.42)	32.6 (0.97)	26.2 (2.29)	25.2 (1.23)	
<b>Width of pronotum</b> <sup>†</sup>	7.4 (0.51)	7.5 (0.45)	5.7 (0.42)	5.7 (0.39)	
<b>Width of abdomen</b> <sup>†</sup>	12.8 (1.31)	11.9 (1.03)	8.7 (0.97)	8.4 (0.54)	
<b>Head length</b> <sup>†</sup>	5.4 (0.33)	5.3 (0.19)	4.5 (0.33)	4.5 (0.18)	
<b>Width across eyes</b>	2.5 (0.23)	2.6 (0.10)	2.2 (0.15)	2.1 (0.10)	
<b>Length of pronotum</b> <sup>†</sup>	4.9 (0.32)	5.1 (0.25)	3.9 (0.39)	3.9 (0.16)	
<b>Ante ocular region</b>	3.0 (0.25)	2.8 (0.08)	2.5 (0.07)	2.3 (0.14)	
<b>Post ocular region</b>	0.8 (0.13)	0.8 (0.08)	0.8 (0.06)	0.8 (0.10)	
<b>Width of eye</b>	0.7 (0.11)	0.8 (0.04)	0.6 (0.07)	0.6 (0.07)	
<b>Synthlipsis</b>	1.0 (0.09)	0.9 (0.06)	0.9 (0.11)	0.9 (0.10)	
<b>Antennae</b>	1 <sup>st</sup> antennomere	1.4 (0.14)	1.4 (0.11)	0.9 (0.08)	1.1 (0.08)
	2 <sup>nd</sup> antennomere	4.4 (0.42)	4.8 (0.36)	4.0 (0.46)	4.3 (0.16)
	3 <sup>rd</sup> antennomere	3.8 (0.16)	3.6 (0.27)	3.6	3.3
	4 <sup>th</sup> antennomere	3.0 (0.31)	3.0 (0.30)	0.0	2.8
	1 <sup>st</sup> article	1.9 (0.23)	1.8 (0.17)	1.9 (0.14)	1.8 (0.24)
<b>Labium</b>	2 <sup>nd</sup> article	3.5 (0.17)	3.5 (0.25)	2.8 (0.20)	2.8 (0.17)
	3 <sup>rd</sup> article	0.97 (0.05)	0.9 (0.11)	0.8 (0.03)	0.9 (0.10)
<b>n</b>	<b>15</b>	<b>10</b>	<b>8</b>	<b>11</b>	

<sup>†</sup>Statistically significant difference between *T. huehuetenanguensis* and *T. dimidiata* s. str. ( $p < 0.01$ , unpaired t-test). Standard deviation is in parenthesis.

Head dark brown with scarce yellow pilosity and overall smooth surface; central band with very shallow rugosity. Head length, male 4.1–4.7 mm, female 4.0–4.8 mm. Ocelli large, lighter than tegument, placed on a pronounced tubercle. Antenniferous tubercles subcylindrical, very short, situated in the middle of the anteocular region; first antennomere not attaining apex of head. Second antennomere lighter than first, with long setae. Ratio of antennomeres I–IV 1:3.9–4.4:3–4:2.5. Apex of clypeus distinctively lighter than rest of head. Labium (Fig. 3) slender, first article reaching level of apex of antenniferous tubercle; second article exceeding posterior border of head, attaining neck; third article light brown, with interarticular areas light yellow (Fig. 3). Ratio of labial articles 1: 1.6:0.5. Most labial setae short, not very numerous on first and second article. Third labial article reaching first third of stridulatory sulcus on males, half on females. Neck dark brown, with very smooth surface, and a pair of lateral yellowish spots.

Pronotum brown, with humerus blunt and pointed, usually lighter in color. Anterolateral angles short, almost round, laterally oriented, almost perpendicular to neck. Submedian carinae very pronounced, with tubercle aspect. Scutellum triangular, shallowly rugose, with the central area distinctly depressed, apical process sometimes lighter in color. (Fig. 4).

Hemelytra not reaching apex of the abdomen, darker at membrane, with scarce light yellow pilosity, dark brown spots around the intersection of the claval suture and

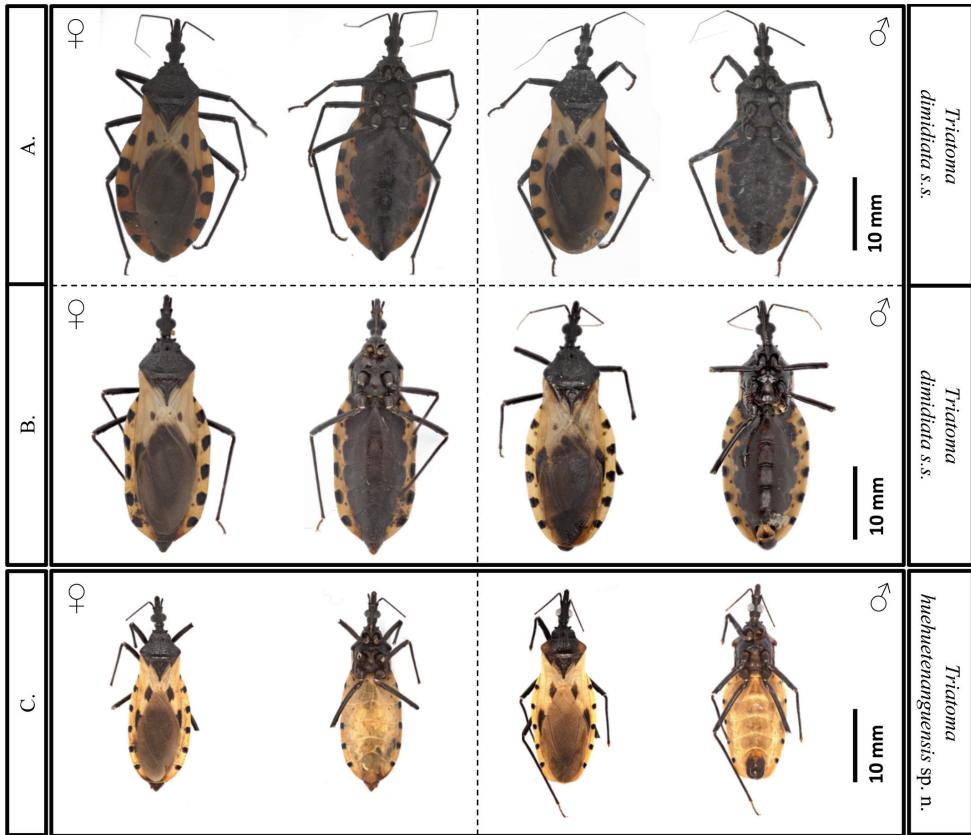


**Figure 2.** Comparison between *T. dimidiata* s. str. and *T. huehuetenanguensis* sp. n. **A** *T. dimidiata* female (left) and male (right) from Jutiapa (dorsal and ventral view) **B** *T. dimidiata* female (left) and male (right) from Huehuetenango (dorsal and ventral view) and **C** *T. huehuetenanguensis* sp. n. female (left) and male (right) from Huehuetenango (dorsal and ventral view). Photograph credits: RL and SJ.

the cubital vein, and two larger dark brown spots: one covering the posterior portion of the cubital and medial veins, and the other (largest) covering the joining of the radial and subcostal veins.

Abdomen ventrally convex, shortly pilose, yellow to light yellow (Fig. 3). Spiracles adjacent, but not touching connexival suture, not very pronounced, concolorous with rest of tegument. Connexival segments with a piceous or black spot covering the entire width of the anterior third, yellow posteriorly (Fig. 5).

Males terminalia almost square-shaped, darker than the rest of the body, with scarce dark pilosity. The posterior margin of urosternite VIII almost straight. Posterior margin of urosternite IX slightly sinuous and not exceeding the abdomen. Female external terminalia triangle-shaped, pale, with very dark, dense pilosity (Fig. 6). Posterior margin of sternite VII very sinuous; gonocoxite VIII (Gc8) pointed; gonapophysis VIII (Gp8) is wider than long. Gonocoxite IX (Gc9) strongly expanded exceeding the abdomen in *T. huehuetenanguensis* (Fig. 6).

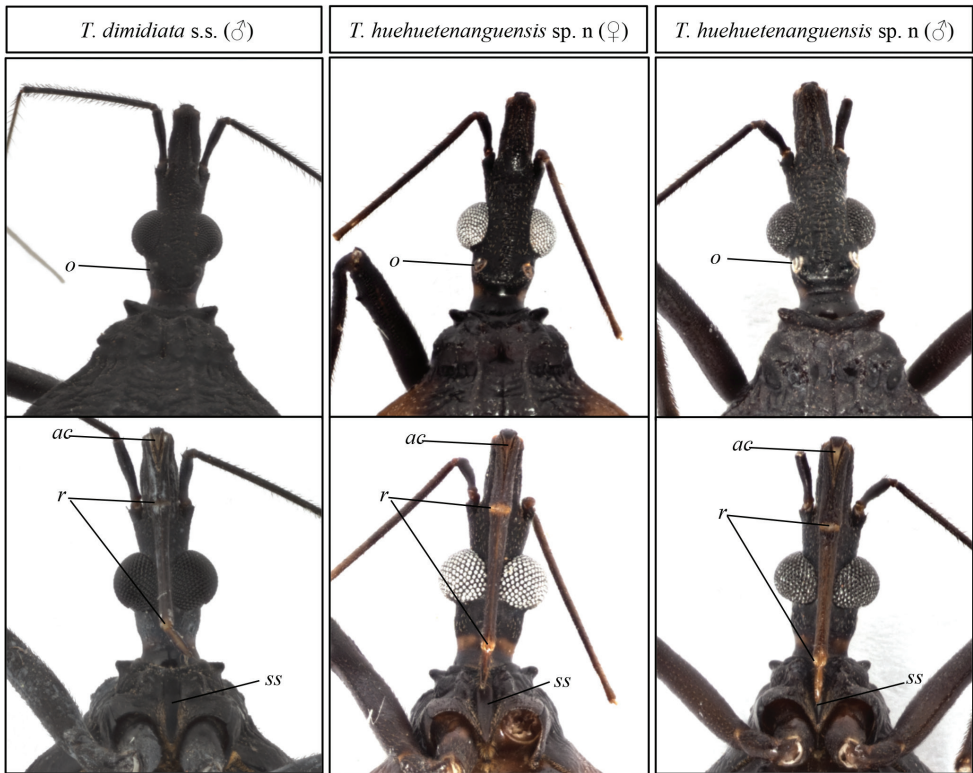


**Figure 3.** Heads of *T. dimidiata* s. str. and *T. huehuetenanguensis* sp. n. Top panel, dorsal view of the head. Bottom panel, ventral view of the head. Abbreviations: **o** ocelli, **ac** apex of clypeus, **ss** stridulatory sulcus, **r** connections between rostral segments. Photograph credits RL and SJ.

**Distribution.** Holotype and paratypes specimens of *T. huehuetenanguensis* were obtained by community participation and reported to be found in domestic environments, near to tropical forest. Huehuetenango is at the northwest of Guatemala and is characterized by pine forest. The altitude ranges from 300 to >3,000 m above sea level. Other localities (Table 1 and Fig. 1) were inferred from specimens collected for previously published molecular phylogenetics studies (Bargues et al. 2008, Dorn et al. 2016, Justi et al. 2018).

**Host-parasite data.** 18 out of the 20 specimens tested were found to be infected with *Trypanosoma cruzi*.

**Discussion.** The ecological diversity within the subfamily Triatominae (>150 species) and its wide distribution through the Americas, and particularly Latin America, have made it difficult to control vector-borne transmission of Chagas disease (WHO 2002). *Triatoma dimidiata* is one of the main vector taxa involved in Chagas transmission in Latin America, specifically the main vector for Central America and a secondary vector in Mexico and Colombia. Its broad geographic range and phylogenetic diversity have posed taxonomic challenges for many years (Dorn et al. 2007). Therefore, understanding the taxonomy, phylogenetic and ecological diversity of the *T. dimidiata* complex is important for understanding *T. cruzi* transmission.

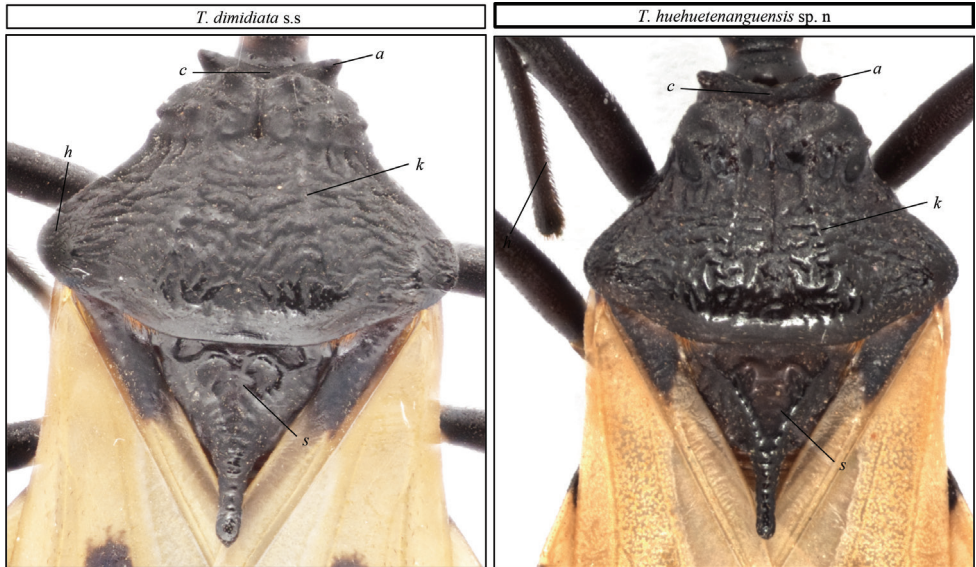


**Figure 4.** Pronotum of *T. dimidiata* s. str. (left), and *T. huehuetenanguensis* sp. n. (right). Abbreviations: c collar, a anterolateral angles, h humerus and s scutellum. Photograph credits RL and SJ.



**Figure 5.** Ventral connexival plate and part of 4<sup>th</sup> urosternite of *T. dimidiata* s. str. (left), and *T. huehuetenanguensis* sp. n. (right). Abbreviations: cs connexival suture and s spiracles. Photograph credits RL and SJ.

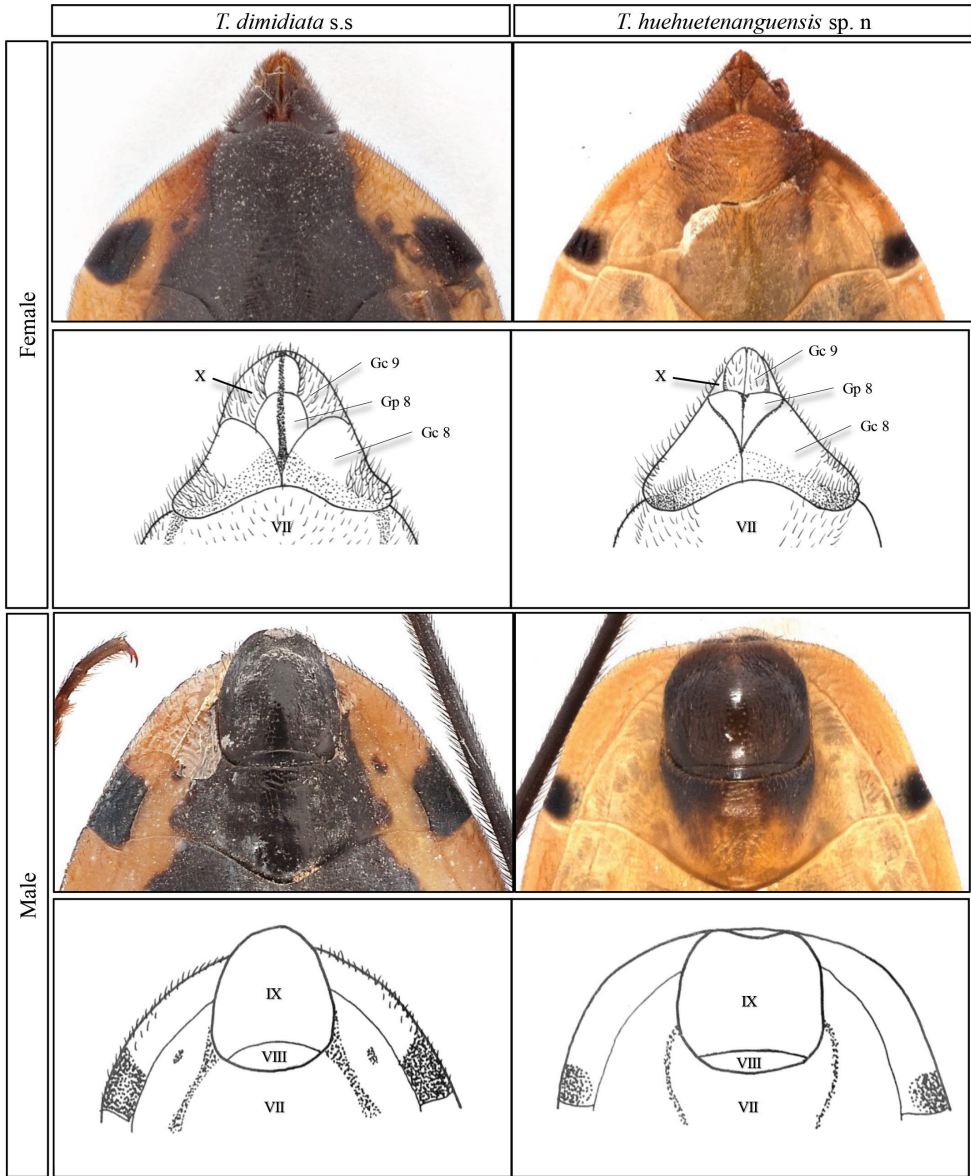


**Figure 6.** Comparison between the external terminalia of *T. dimidiata* s. str. and *T. huehuetenanguensis* sp. n. Abbreviations: **Gc 8** gonocoxite VIII; **Gc 9** gonocoxite IX; **Gp8** gonapophysis VIII; **VII** sternite; **IX** and **X** segments. Drawings RL. Photograph credits RL and SJ.

Here we are presenting three lines of evidence that support *T. huehuetenanguensis* as a distinct species: morphological, nuclear genetic (ITS-2) and mitochondrial genetic (cytB). The morphological characters included in the taxonomic key for *Triatoma* species (Lent and Wygodzinsky 1979) for *T. dimidiata* encompass *T. huehuetenanguensis*, specifically overall size and measurements of the head and

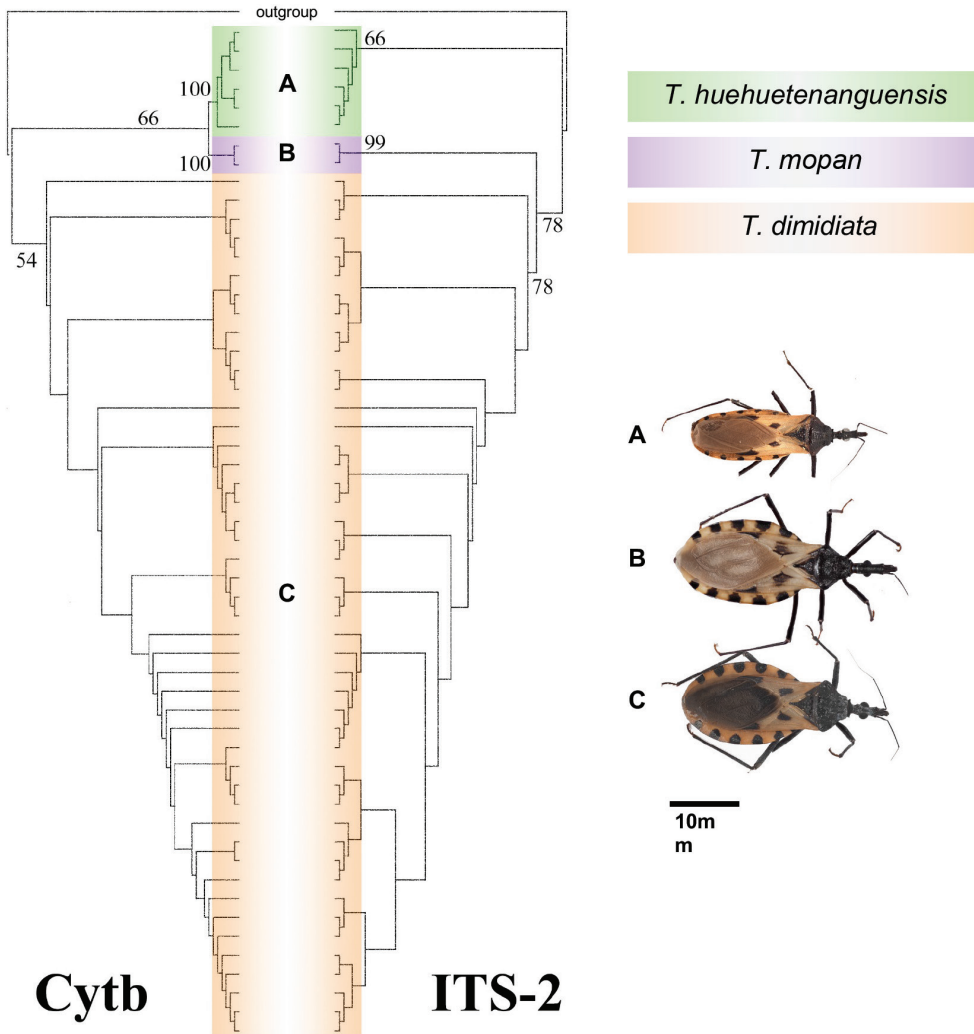


**Figure 7.** Maximum likelihood cytb and ITS-2 phylogenies. Bootstrap support values of the relevant clades are shown. Habitus of *T. huehuetenanguensis* and related species are shown to scale (10 mm).

eyes. However, on closer examination, macroscopic differences, including those summarized in Table 4, reveal *T. huehuetenanguensis* as morphologically different. Color differentiation on connexivum, pilosity, ocelli, labial articles joints, and female and male terminalia separate *T. huehuetenanguensis* from *T. dimidiata*. Differentiation based on the color pattern of the connexivum and other body regions was used in the description of *T. brailovskyi* (Martinez, Carcavallo & Pelaez, 1984), *T. gomeznunezi* (Martinez, Carcavallo & Jurberg, 1994) and most recently *Triatoma mopan* (Dorn et al., 2018). This latter study attributed the diminished pigmentation of *T. mopan* as the result to the cave environment. In our case, where both, *T. huehuetenanguensis* and *T. dimidiata* are found in sympatry and in domestic environments, it would be

**Table 4.** Ten distinguishing features between *T. dimidiata* and *T. huehuetenanguensis* sp. n.

Feature	<i>Triatoma dimidiata</i> <sup>†</sup>	<i>Triatoma huehuetenanguensis</i> sp. n
<b>Connexivum overall color</b>	Dorsal part is pale yellow to orange yellow, and the ventral part is brown to black	Dorsal and ventral sides are yellow to light yellow
<b>Color of head pilosity</b>	Dark colored	Light yellow
<b>Ocelli</b>	Dark colored	Light colored, implanted in a very pronounced tubercle
<b>Setae in the 2<sup>nd</sup> antennomere</b>	Abundant	Scarce
<b>Anterolateral angles</b>	Anteriorly oriented, short and sub conical	Laterally oriented, almost perpendicular to the neck, very short and rounder
<b>Labial articles</b>	Joint dark colored	Joint yellow colored
<b>Setae in the abdomen</b>	Abundant and dark colored	Scarce and yellow colored
<b>Spiracles</b>	Close but not touching the connexival suture. Surrounded by a dark spot on the tegument.	Adjacent, but not touching the connexival suture. Same color as the tegument.
<b>Female external terminalia</b>	Triangle-shaped with rounded apex	Triangle-shaped with pointed apex
<b>Male external terminalia</b>	Ovoid shape	Square-shaped
	Limit of the 8 <sup>th</sup> urosternite is curved	Limit of the 8 <sup>th</sup> urosternite is straight

<sup>†</sup> *T. dimidiata* features are based on Lent and Wygodzinsky (1979) and *T. dimidiata* s. str. (group 1–2) specimens from Jutiapa, Guatemala.

interesting to determine the process that caused such color differentiation between these two species. Another important morphological character is the location and pigmentation of the spiracles. These structures in *T. huehuetenanguensis* are adjacent to the connexival suture, whereas in *T. dimidiata*, they are close but not adjacent to the connexival suture. Differentiation based on the location and color of the respiratory spiracles was reported in the description of *Rhodnius montenegrensis* (Rosa et al. 2012) and most recently in the description of *Triatoma mopan* (Dorn et al., 2018).

The phylogenetic molecular analysis from the nuclear ITS-2 and the mitochondrial cytb gene, recovered a single monophyletic clade with high support (Fig. 7), and low genetic divergence (<3.1% for cytb and < 0.6% for ITS-2) indicating that *Triatoma dimidiata* auct., non (Latreille, 1811), *Triatoma* sp. aff. *dimidiata* (Bargues et al. 2008), *Triatoma* sp. aff. *dimidiata* group 3 (Monteiro et al. 2013, Dorn et al. 2016, Justi et al. 2018) and *T. huehuetenanguensis* are the same species (see Suppl. material 3: cytb maximum likelihood phylogeny and Suppl. material 4: ITS-2 maximum likelihood phylogeny). Previously published molecular phylogenies (Bargues et al. 2008, Monteiro et al. 2013, Dorn et al. 2016, Justi et al. 2018) have thoroughly described the ITS-2 and cytb diversity within and among the four groups that comprise *T. dimidiata* s. l. This allowed us to compare these two regions in two of the specimens used by Justi et al. (2018), and verify that they fall within the monophyletic clade. Two Triatominae species were differentiated based on molecular analysis of the mitochondrial gene (Cytb), *R. montenegrensis* (Da Rosa et al. 2012) and *Rhodnius marabaensis* (Souza et al. 2016).

As supported by our genetic data, we suggest the inclusion of *T. huehuetenanguensis* in the subcomplex *T. dimidiata*. Based on Justi and Galvao (2017), this subcomplex

**Table 5.** Distinguishing features between the species of *T. dimidiata* subcomplex based on Justi and Galvão (2017). This reference was used as the original description is not very detailed, and Lent and Wygodzinsky (1979) provide a much more detailed description of the morphology upon inspection of 160 specimens.

Species	Reference	Features
<i>T. dimidiata</i>	Lent and Wygodzinsky (1979)*	First antennae segment attaining level of apex of clypeus; anterolateral angles anterolaterally directed; central area of the scutellum not depressed; spiracles close but not adjacent to connexival suture, connexivum dark.
<i>T. hegneri</i>	Lent and Wygodzinsky (1979)	Labium very short; abdomen flattened below with spiracles distant from connexival suture; venter and connexivum uniformly dark.
<i>T. brailovskyi</i>	Martinez et al. (1984)	Overall size small with very large eyes and ocelli, pronotum with an evident keel at the border, anterolateral angles short and subconical, fore and mid femora with 1 + 1 subapical denticles.
<i>T. gomeznunezi</i>	Martinez et al. (1994)	Antenniferous tubercle laterally covered with long setae and dorsally glabrous; neck polished and entirely black; corium dark brown with two basal and distal yellowish spots; venter convex but longitudinally flattened; venter black.
<i>T. mopan</i>	Dorn et al. (2018)	Pronotum without discal tubercles and presenting a straight latitudinal depression dividing it in half, fore-femora with 1+1 apical, small denticles, 2 +1 subapical denticles in both males and females; and 1+1 apical, small denticles, 2 +2 asymmetrical subapical larger denticles on males and 2 +2 larger, asymmetrical subapical denticles on females, and spiracles close adjacent to connexival suture, surrounded by a spot slightly darker than the tegument
<i>T. huehuetenanguensis</i>	This study	Short yellow pilosity in the whole body except in the genitalia; connections between each segment of the labium are very visible and light-yellow colored; color of venter light yellow.

is comprised by: *T. dimidiata*, *T. hegneri*, *T. brailovskyi* and *T. gomeznunezi*, and more recently *T. mopan* has been added (Dorn et al. 2018). The most relevant differences between these six species are summarized in Table 5.

Relevant Triatominae species for human *T. cruzi* transmission are those that have evolved to live close to humans and have been found to be infected *T. cruzi* (WHO 2002). *Triatoma huehuetenanguensis* was collected in both peridomestic and intradomestic environments. The high natural infection with *T. cruzi* (> 90% of the specimens) suggests it is a potentially important vector and its role in human Chagas disease should be further evaluated.

## Acknowledgements

Salvador Castellanos at the Applied Entomology and Parasitology Laboratory (LENAP) for insect preservation. Lisa Chamberland and Laura Caicedo at the University of Vermont (UVM) for support and help with the Visionary Digital BK Laboratory System. Sara Cahan (UVM) for use of the Nikon stereoscope Model SMZ-1B. The personnel

of the Ministry of Health of Huehuetenango, especially to Mirna Sosa for their help in field collections. The reviewers who helped greatly improve this manuscript.

This manuscript was prepared in part while SAJ held a Postdoctoral fellowship from the National Science Foundation (NSF) grant BCS-1216193 as part of the joint NSF-NIH-USDA (United States Department of Agriculture) Ecology and Evolution of Infectious Diseases program; and, in part as a National Research Council Research Associate Awardee at the Walter Reed Army Institute of Research. The material published reflects the views of the authors and should not be construed to represent those of the Department of the Army, the Department of Defense or the Department of Agriculture.

**Financial Support:** This work was supported with a subsidy of the Ecohealth Initiative Program of the Center of Investigations for the Development of Canada (IDRC; <http://www.idrc.ca/ecohealth>) (Subsidy no 106531) to Carlota Monroy; a grant from the World Health Organization (Tropical Disease Research-World Health Organization grant, TDR –WHO ID# A10249) awarded to CM, by National Science Foundation (NSF) grant BCS-1216193 as part of the joint NSF-NIH-USDA (United States Department of Agriculture) Ecology and Evolution of Infectious Diseases program to CM, PD and LS and grant R03AI26268/1-2 from the National Institute of Allergy and Infectious Disease (NIAID) of the National Institutes of Health (NIH) to LS.

## References

- Bargues MD, Klisiowicz DR, Gonzalez-Candelas F, Ramsey JM, Monroy C, Ponce C, Salazar-Schettino PM, Panzera F, Abad-Franch F, Sousa OE, Schofield CJ, Dujardin JP, Guhl F, Mas-Coma S (2008) Phylogeography and genetic variation of *Triatoma dimidiata*, the main Chagas disease vector in Central America, and its position within the genus *Triatoma*. *PLoS Neglected Tropical Diseases* 2(5): e233. <https://doi.org/10.1371/journal.pntd.0000233>
- Becker RWA, Wilks AR (2018) Package “maps”: Draw Geographical Maps. R package version (>=3.0.0). <http://CRAN.R-project.org/package=maps>
- Chagas C (1909) Nova tripanozomíaze humana: estudos sobre a morfologia e o ciclo evolutivo do *Schizotrypanum cruzi* n. gen., n. sp., agente etiológico de nova entidade morbida do homem. *Memórias do Instituto Oswaldo Cruz* 1(2): 159–218. <https://doi.org/10.1590/S0074-02761909000200008>
- Dorn PL, de la Rúa NM, Axen H, Smith N, Richards BR, Charabati J, Suarez J, Woods A, Pessoa R, Monroy C, Kilpatrick W, Stevens L (2016) Hypothesis testing clarifies the systematics of the main Central American Chagas disease vector, *Triatoma dimidiata* (Latreille, 1811), across its geographic range. *Infection Genetics and Evolution* 44: 431–443. <https://doi.org/10.1016/j.meegid.2016.07.046>
- Dorn PL, Monroy C, Curtis A (2007) *Triatoma dimidiata* (Latreille, 1811): a review of its diversity across its geographic range and the relationship among populations. *Infection Genetics and Evolution* 7(2): 343–352. <https://doi.org/10.1016/j.meegid.2006.10.001>

- Guindon S, Gascuel O (2003) A simple, fast, and accurate algorithm to estimate large phylogenies by maximum likelihood. *Systematic Biology* 52(5): 696–704. <https://doi.org/10.1080/10635150390235520>
- Hijmans R, van Etter J (2012) Raster: Geographic analysis and modeling with raster data. R package version 2.0–12.
- Justi SA, Cahan S, Stevens L, Monroy C, Lima-Cordon R, Dorn PL (2018) Vectors of diversity: Genome wide diversity across the geographic range of the Chagas disease vector *Triatoma dimidiata* sensu lato (Hemiptera: Reduviidae). *Molecular Phylogenetics and Evolution* 120: 144–150. <https://doi.org/10.1016/j.ympev.2017.12.016>
- Justi SA, Galvao C (2017) The Evolutionary Origin of Diversity in Chagas Disease Vectors. *Trends in Parasitology* 33(1): 42–52. <https://doi.org/10.1016/j.pt.2016.11.002>
- Katoh K, Rozewicki J, Yamada KD (2017) MAFFT online service: multiple sequence alignment, interactive sequence choice and visualization. *Briefings in Bioinformatics*. <https://doi.org/10.1093/bib/bbx108>
- Larkin MA, Blackshields G, Brown NP, Chenna R, McGettigan PA, McWilliam H, Valentin F, Wallace IM, Wilm A, Lopez R, Gibson TJ, Higgins DG (2007) Clustal W and Clustal X version 2.0. *Bioinformatics* 23(21): 2947–2948. <https://doi.org/10.1093/bioinformatics/btm404>
- Lent H, Wygodzinsky P (1979) Revision of the Triatominae (Hemiptera, Reduviidae), and their significance as vectors of Chagas' disease. *Bulletin of the American museum of Natural History* 163(3): 123–520.
- Martinez A, Carcavallo RU, Jurberg J (1994) *Triatoma gomeznunezi* a new species of Triatomini from Mexico (Hemiptera, Reduviidae, Triatominae). *Entomología y Vectores* 1: 15–19.
- Martinez A, Carcavallo RU, Pelaez D (1984) *Triatoma brailovskyi* nueva especie de Triatominae de Mexico. *Chagas* 1(2): 39–42.
- Monteiro FA, Peretolchina T, Lazoski C, Harris K, Dotson EM, Abad-Franch F, Tamayo E, Pennington PM, Monroy C, Cordon-Rosales C, Salazar-Schettino PM, Gómez-Palacio A, Grijalva MJ, Beard CB, Marcet PL (2013) Phylogeographic pattern and extensive mitochondrial DNA divergence disclose a species complex within the Chagas disease vector *Triatoma dimidiata*. *PLoS ONE* 8(8): e70974. <https://doi.org/10.1371/journal.pone.0070974>
- Paradis E, Claude J, Strimmer K (2004) APE: Analyses of Phylogenetics and Evolution in R language. *Bioinformatics* 20(2): 289–290. <https://doi.org/10.1093/bioinformatics/btg412>
- Da Rosa JA, Rocha CS, Gardim S, Pinto MC, Mendonca VJ, Ferreira Filho JCR, Oliveira Costa de Carvalho E, Aranha Camargo LM, De Oliveira J, Nascimento JD, Cilense M, Almeida CE (2012) Description of *Rhodnius montenegrensis* n. sp. (Hemiptera: Reduviidae: Triatominae) from the state of Rondônia, Brazil. *Zootaxa* 3478: 62–76.
- Schofield CJ, Galvao C (2009) Classification, evolution, and species groups within the Triatominae. *Acta Tropica* 110(2–3): 88–100. <https://doi.org/10.1016/j.actatropica.2009.01.010>
- Souza ED, Von Atzingen NC, Furtado MB, de Oliveira J, Nascimento JD, Vendrami DP, Gardim S, da Rosa JA (2016) Description of *Rhodnius marabaensis* sp. n. (Hemiptera, Reduviidae)

dae, Triatominae) from Para State, Brazil. *ZooKeys* 621: 45–62. <https://doi.org/10.3897/zookeys.621.9662>

Tamura K, Stecher G, Peterson D, Filipski A, Kumar S (2013) MEGA6: molecular evolutionary genetics analysis version 6.0. *Molecular biology and evolution* 30(12): 2725–2729. <https://doi.org/10.1093/molbev/msw054>

Team RC (2013) R: A language and environment for statistical computing.

WHO (2002) Control of Chagas disease: Second report of the WHO Expert Committee (Vol. 2): World Health Organization.

WHO (2015) Chagas disease in Latin America: an epidemiological update based on 2010 estimates. *Weekly Epidemiological Record / Relevé épidémiologique hebdomadaire* 90(06): 33–44.

Wickham H (2011) The split-apply-combine strategy for data analysis. *Journal of Statistical Software* 40(1): 1–29. <https://doi.org/10.18637/jss.v040.i01>

## **Supplementary material 1**

### **Morphological measurements**

Authors: Raquel Asunción Lima-Cordón, María Carlota Monroy, Lori Stevens, Antonieta Rodas, Gabriela Anaité Rodas, Patricia L. Dorn, Silvia A. Justi

Data type: species data

Copyright notice: This dataset is made available under the Open Database License (<http://opendatacommons.org/licenses/odbl/1.0/>). The Open Database License (ODbL) is a license agreement intended to allow users to freely share, modify, and use this Dataset while maintaining this same freedom for others, provided that the original source and author(s) are credited.

Link: <https://doi.org/10.3897/zookeys.820.27258.suppl1>

## **Supplementary material 2**

### **Script Huehuetenango map**

Authors: Raquel Asunción Lima-Cordón, María Carlota Monroy, Lori Stevens, Antonieta Rodas, Gabriela Anaité Rodas, Patricia L. Dorn, Silvia A. Justi

Data type: occurrence

Copyright notice: This dataset is made available under the Open Database License (<http://opendatacommons.org/licenses/odbl/1.0/>). The Open Database License (ODbL) is a license agreement intended to allow users to freely share, modify, and use this Dataset while maintaining this same freedom for others, provided that the original source and author(s) are credited.

Link: <https://doi.org/10.3897/zookeys.820.27258.suppl2>

### **Supplementary material 3**

#### **CytB maximum likelihood phylogeny**

Authors: Raquel Asunción Lima-Cordón, María Carlota Monroy, Lori Stevens, Antonieta Rodas, Gabriela Anaité Rodas, Patricia L. Dorn, Silvia A. Justí

Data type: phylogeny data

Copyright notice: This dataset is made available under the Open Database License (<http://opendatacommons.org/licenses/odbl/1.0/>). The Open Database License (ODbL) is a license agreement intended to allow users to freely share, modify, and use this Dataset while maintaining this same freedom for others, provided that the original source and author(s) are credited.

Link: <https://doi.org/10.3897/zookeys.820.27258.suppl3>

### **Supplementary material 4**

#### **ITS2 maximum likelihood phylogeny**

Authors: Raquel Asunción Lima-Cordón, María Carlota Monroy, Lori Stevens, Antonieta Rodas, Gabriela Anaité Rodas, Patricia L. Dorn, Silvia A. Justí

Data type: phylogeny data

Copyright notice: This dataset is made available under the Open Database License (<http://opendatacommons.org/licenses/odbl/1.0/>). The Open Database License (ODbL) is a license agreement intended to allow users to freely share, modify, and use this Dataset while maintaining this same freedom for others, provided that the original source and author(s) are credited.

Link: <https://doi.org/10.3897/zookeys.820.27258.suppl4>